Journal of Alloys and Compounds 509 (2011) 1595–1600

Contents lists available at ScienceDirect

Journal of Alloys and Compounds

journal homepage: www.elsevier.com/locate/jallcom

Lead-free soldering: Investigation of the Cu–Sn–Sb system along the Sn:Sb = 1:1 isopleth

Y. Yuan [a,b], G. Borzone [b,*], G. Zanicchi [b], S. Delsante [b]

[a] State Key Laboratory of Powder Metallurgy, Central South University, Changsha, Hunan 410083, PR China
[b] Department of Chemistry and Industrial Chemistry, University of Genoa, INSTM UdR Genoa, Via Dodecaneso 31, I-16146 Genoa, Italy

ARTICLE INFO

Article history:
Received 17 August 2010
Received in revised form 28 October 2010
Accepted 28 October 2010
Available online 9 November 2010

Keywords:
Lead-free solders
Differential scanning calorimetry
Cu–Sn–Sb
Phase diagram

ABSTRACT

The Cu–Sn–Sb system has been experimentally investigated by a combination of optical microscopy, differential scanning calorimetry (DSC) and electron probe microanalysis (EPMA). DSC was used to identify a total number of five invariant ternary reactions and the Sn:Sb = 1:1 isopleth section up to 65 at.% Cu was constructed by combining the DSC data with the EPMA analyses of annealed alloys and literature information. The composition limits of the binary phases were detected.

1. Introduction

As one of the basic systems of the bearing metals and Britannia metals, Cu–Sn–Sb system has attracted extensive attention since the beginning of the 20th century [1–9]. The status of investigations available and a thorough analysis of earlier phase relation descriptions for the Cu–Sn–Sb system was made in recent critical assessment by Ghosh [9], where the majority of all literature data up to 1995 was included. Systematic investigations were performed in the past [4,6] using metallographic and thermal analysis. Harding and Pell-Walpole [7] investigated the phase equilibria in the Sn-rich corner and reported isothermal sections between 20 and 240 °C. After the 1950s, there are little experimental investigations on this system. Today there is a renewed interest in the Cu–Sn–Sb system and its phase equilibria and phase transformations because of its soldering application in the electronic industry. Lead-free solder interconnect reliability is a very complex issue, and it depends on many factors. The 'mainstream' lead-free solder alloy is Sn–Ag–Cu (SAC) and commercial Castin^{TM} Sn–Ag–Cu–Sb (Sn96.2Ag2.5Cu0.8Sb0.5 mass%) alloys are available and considered to be safe and effective lead-free solders for high temperature applications.

The knowledge of the thermodynamic properties of the Cu–Sn–Sb system has therefore been considered very useful and has been included in the European COST Action MP0602 (Advanced Solder Materials for High Temperature Application). As part of this project, this work is devoted to the experimental investigation of the phase transformations along the Sn:Sb = 1:1 isopleth by differential scanning calorimetry (DSC) and microscopic analyses.

In the framework of the European COST Action MP0602, thermodynamic properties of Cu–Sb–Sn liquid alloys have also been studied by Romanowska using the equilibrium saturation method [10].

Using two different types of high temperature drop calorimeters, partial and integral enthalpies of mixing of liquid alloys were determined in the ternary Cu-Sb-Sn system by Jendrzejczyk-Handzlik et al. [11].

2. Experimental

All the alloys were prepared by repetitive induction melting followed by air cooling of pure Sn, Sb, and Cu rods produced by NewMet Koch company with a purity of 99.999 mass%. Cu was cleaned in a H_2-flow at 150 °C for 2 h to remove the oxide.

The raw materials have been weighed according to the selected compositions with a total amount of 2 g and sealed in cleaned quartz tubes under Ar.

The alloy buttons were divided into several pieces. One piece with around 0.5 g weight was sealed in the special-made quartz crucible for differential scanning calorimetric (DSC) analysis. Remaining portions were sealed in quartz tubes and annealed at selected temperatures for long periods, followed by quenching in icy-water.

The DSC111 SETARAM apparatus designed as a Calvet calorimeter (where the cylindrical reference and working cells are surrounded by two differentially connected thermal fluximeters) was used in a continuous mode. An empty quartz crucible having a weight as close as possible to the quartz crucible holding the sample was used as reference. Generally, all samples were heated and cooled in two different cycles from 150 °C up to and over the melting temperature with scanning rate of 1 °C/min, followed by a 2nd run at 0.5 °C/min. Because of the limited temperature range of the operation of the DSC employed (highest temperature 800 °C), the measurements along the Sn:Sb = 1:1 isopleth were performed for compositions up to 65 at.% Cu.

---

* Corresponding author. Tel.: +39 0103536153; fax: +39 0103538733.
E-mail address: borzone@chimica.unige.it (G. Borzone).

0925-8388/$ – see front matter © 2010 Elsevier B.V. All rights reserved.
doi:10.1016/j.jallcom.2010.10.186

Table 1
Cu–Sn–Sb alloys. Experimental DSC results and SEM–EDS composition.

Sample	EDS composition (at.%)	Heating run, *T* (°C)	Cooling run, *T* (°C)	Reaction	Remarks
CSS1		150 °C ↔ 500 °C × 1/0.5 °C/min			
	Cu, 9.0	236/237	235/234	U5	S.E.
	Sn, 46.0	309/308	304/304	U4	S.E.
	Sb, 45.0	368/367	367/367	U3	
		383/382	373/374		
		399/399	397/397	Liquidus	
CSS2		200 °C ↔ 550 °C × 1/0.5 °C/min			
	Cu, 19.5	236/236	235/235	U5	S.E.
	Sn, 40.4	310/311	304/304	U4	S.E.
	Sb, 40.1	368/368	366/365	U3	
		381/377	377/377		
		418/424	417/418	Liquidus	
CSS3		150 °C ↔ 700 °C × 1/1 °C/min			
	Cu, 30.0	236/236	235/235	U5	S.E.
	Sn, 35.0	310/310	304/307	U4	S.E.
	Sb, 35.0	368/369	365/357	U3	
		458/465	450/449	Liquidus	
CSS10		200 °C ↔ 600 °C × 1/0.5 °C/min			See Fig. 1a
	Cu, 33.8	236/236	236/235	U5	S.E.
	Sn, 32.7	310/309	301/305	U4	S.E.
	Sb, 33.5	368/368	365/365	U3	
		382/380	372/373		S.E.
		475/480	467/466	Liquidus	
CSS4		200 °C ↔ 700 °C × 1/0.5/0.5 °C/min			
	Cu, 37.0	236/237/237	235/234	U5	S.E.
	Sn, 31.6	310/310/308	302/305	U4	S.E.
	Sb, 31.4	369/368/369	364/363	U3	
		–/388/390	401/397		
		478/477/481			
		495/496/495	481/480	Liquidus	
CSS9		200 °C ↔ 600 °C × 1/0.5 °C/min			
	Cu, 47.0	369/369	367/367	U3	
	Sn, 26.5	408/407	404/404	U2	
	Sb, 26.5		466/467		
		478/477	468/469	U1	
		508/506			
		549/550	530/530	Liquidus	
CSS5		150 °C ↔ 700 °C × 0.5 °C/min			
	Cu, 48.0	369	367	U3	
	Sn, 26.0	408	405	U2	
	Sb, 26.0	478	473	U1	
		515			
		554	532	Liquidus	
CSS6		200 °C ↔ 750 °C × 0.5 °C/min			See Fig. 1c
	Cu, 50.0	368	367	U3	
	Sn, 25.5	407	405	U2	
	Sb, 24.5	478	468	U1	
		515			
		564	551	Liquidus	
CSS7		200 °C ↔ 750 °C × 1/0.5 °C/min			See Fig. 3b
	Cu, 57.0	368/368	366/366	U3	S.E.
	Sn, 21.8	407/407	405/405	U2	
	Sb, 21.2	477/478	468/468	U1	
		–/522			
		595/595	584/582	Liquidus	
CSS8		300 °C ↔ 750 °C × 1 °C/min			See Fig. 1b
	Cu, 64.3	406	405	U2	
	Sn, 17.6	477	463	U1	
	Sb, 18.1	526			
		631	615	Liquidus	

S.E. = small effect.

Microstructural observations were made on the mechanically polished samples to 1 μm diamond past with light optical microscope (LOM, Leica DM4000) and back scattered electron (BSE) or secondary electron (SE) images using a scanning electron microscopy (SEM) Zeiss-EVO 40.

Quantitative data were collected at 20 kV on a Link System Ltd. Instrument equipped with an energy dispersive spectrometry (EDS) detector. A counting time of 100 s and a ZAF correction program were used. Certified pure elements were used as reference standards, while cobalt was adopted for calibration purposes.

These techniques were used to identify the phases present in the as-cast, as well as the annealed and DSC samples.

3. Results and discussions

In this investigation about 23 alloys have been analysed. The DSC analysis data are summarized in Table 1, together with the

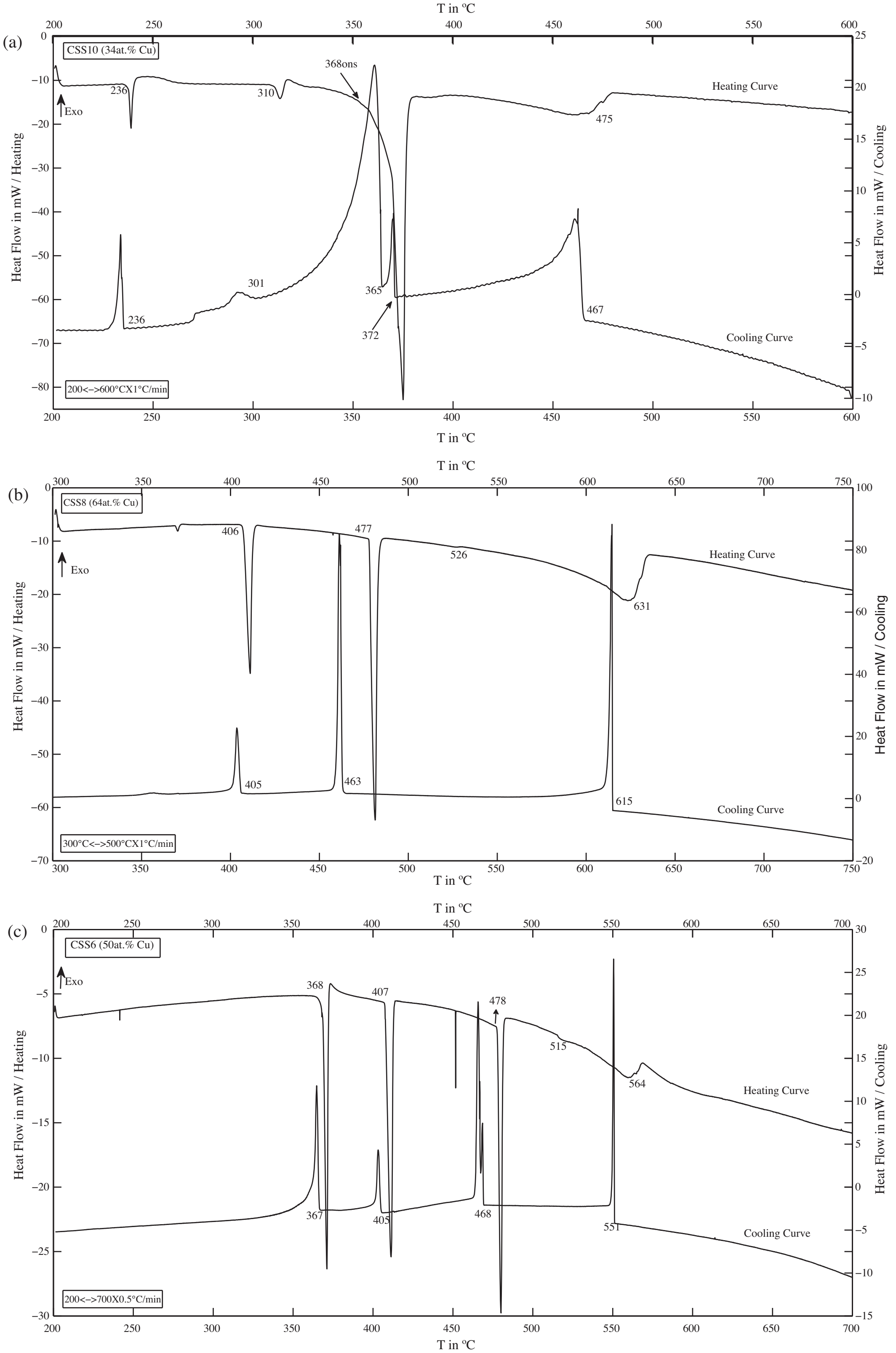

Fig. 1. Cu–Sn–Sb system. DCS heating and cooling traces for selected as-cast samples: (a) CSS10 (33.8 at.% Cu), 1 °C/min rate; (b) CSS8 (64.3 at.% Cu), 1 °C/min rate; (c) CSS6 (50.0 at.% Cu), 0.5 °C/min rate.

composition of the alloys used in the experiment. The temperature values obtained at different rates (1/0.5 °C/min) are reported in the 3rd column for the heating and in the 4th column for the cooling runs, respectively. On heating, the onset temperature of the thermal effect was selected as the temperature of the occurring transformation and the peak temperature of the last thermal event as the liquidus temperature [12]. The good reproducibility of the transformation temperatures and the good agreement between

Table 2
Cu–Sn–Sb system: invariant reaction temperatures determined in this work in comparison with literature data.

Type	Reaction	T (°C); this work	T (°C) [6,9]
U1	$\mathrm{L} + \gamma_1\mathrm{Cu_3(Sb,Sn)} \leftrightarrow \rho(\mathrm{Cu_2Sb}) + \varepsilon(\mathrm{Cu_3Sn})$	478	470
U2	$\mathrm{L} + \varepsilon(\mathrm{Cu_3Sn}) \leftrightarrow \rho(\mathrm{Cu_2Sb}) + \eta(\mathrm{Cu_6Sn_5})$	407	405
U3	$\mathrm{L} + \rho(\mathrm{Cu_2Sb}) \leftrightarrow \beta(\mathrm{SbSn}) + \eta(\mathrm{Cu_6Sn_5})$	368	372
U4	$\mathrm{L} + \beta(\mathrm{SbSn}) \leftrightarrow \mathrm{Sb_2Sn_3} + \eta(\mathrm{Cu_6Sn_5})$	310	319
U5	$\mathrm{L} + \mathrm{Sb_2Sn_3} \leftrightarrow (\beta\mathrm{Sn}) + \eta(\mathrm{Cu_6Sn_5})$	236	240

the values obtained at different rates for the invariant reactions may be observed.

Some examples of the DSC curves for as-cast samples obtained at different heating rates are shown in Fig. 1. Five invariant reactions have been detected; the temperatures listed in Table 2 have been selected at the rate of 1 °C/min. The temperatures assigned are in good agreement with the results reported by Tasaki [6].

In order to determine the exact transformations identified by DSC experiments, the annealed and quenched alloys were used, the results of which are shown in Table 3. The specimens were quenched at selected temperatures above transition temperature U1 (478 °C), between U_1 and U_2 (407 °C) and below the U_2 and U_3 (368 °C) transition temperatures.

The annealed samples characterized by SEM analysis showed a uniform distribution of the phases. Analyses were made at several different locations within each sample, and it was noted that there was very little variation in composition, suggesting that the equilibrium state had been reached. During the quenching, the liquid phase transforms into fine solid phases and an averaged analysis composition is reported. The micrographs in Fig. 2(a)–(f) show the evolved microstructures in the quenched specimen.

From microscopic analysis of these samples, no solubility of copper in the $\beta(\mathrm{SbSn})$ phase was observed (at 350 °C), in agreement with Kamal et al. [13]. In samples annealed at 450 °C a solubility of Sb up to 4.5 at.% in the $\varepsilon(\mathrm{Cu_3Sn})$ and of Sn up to 6 at.% in the $\rho(\mathrm{Cu_2Sb})$ binary phases was determined. A solubility of Sb up to 20 at.% in the $\eta(\mathrm{Cu_6Sn_5})$ phase was detected in samples annealed at 400 °C. No ternary intermetallic phase was found in this work.

Upon consideration of the DSC results in combination with the crystallization path observed in the different alloys, the phase relations detected in the annealed samples and literature information, the five invariant reactions have been identified as shown in Table 2. Fig. 3 shows several typical microphotographs of the samples as-cast and after DSC analysis. Fig. 3a shows the BSE image of the as-cast CSS3 sample with elongated $\rho(\mathrm{Cu_2Sb})$ primary crystals together with the $\beta(\mathrm{SbSn})$ and $\eta(\mathrm{Cu_6Sn_5})$ phases formed during the U3 reaction.

Fig. 3b shows the BSE image of the CSS7 sample after DSC. During the solidification the liquidus first gave the γ_1 $\mathrm{Cu_3(Sb,Sn)}$ primary phase and then went through the sequence of the U1, U2 and U3 invariant reactions. The γ_1 $\mathrm{Cu_3(Sb,Sn)}$ phase has been totally consumed during the U1 reaction forming the $\rho(\mathrm{Cu_2Sb})$ and $\varepsilon(\mathrm{Cu_3Sn})$ phases.

All the DSC curves of samples with a content of Cu < 40 at.% gave two very small thermal effects around 236 °C and 310 °C, as shown for instance in Fig. 1 for the sample CSS10. According to

Table 3
Summary of the phases observed and EDS experimental results of the Cu–Sn–Sb alloys (for the section Sn/Sb = 1:1) annealed and icy-water quenched.

Sample	at.%Cu	Annealing, T (°C)	Annealing time	Remarks	Phases observed	at.%		
						Cu	Sn	Sb
CSS1	9.0	350	40 days	Fig. 2a	$\beta(\mathrm{SbSn})$	0.0	47.7	52.3
					$\eta(\mathrm{Cu_6Sn_5})$	53.4	35.7	10.9
CSS3	30.0	350	40 days		$\beta(\mathrm{SbSn})$	0.0	45.1	55.9
					$\eta(\mathrm{Cu_6Sn_5})$	51.8	29.6	18.6
					$\rho(\mathrm{Cu_2Sb})$	65.0	4.9	30.1
CSS7	57.0	350	40 days		$\eta(\mathrm{Cu_6Sn_5})$	52.6	29.7	17.7
					$\rho(\mathrm{Cu_2Sb})$	65.0	6.3	28.7
					$\varepsilon(\mathrm{Cu_3Sn})$	74.1	20.0	5.9
CSS4	37.0	380	25 days	Fig. 2b	L	~12	~50	~38
					$\eta(\mathrm{Cu_6Sn_5})$	51.7	27.9	20.4
					$\rho(\mathrm{Cu_2Sb})$	65.1	5.2	29.7
CSS7	57.0	400	25 days	Fig. 2c	$\eta(\mathrm{Cu_6Sn_5})$	51.7	28.9	19.3
					$\rho(\mathrm{Cu_2Sb})$	65.4	5.7	28.9
					$\varepsilon(\mathrm{Cu_3Sn})$	75.0	21.3	3.7
CSS6	50.0	400	25 days		L	~12	~50	~38
					$\eta(\mathrm{Cu_6Sn_5})$	51.6	27.6	20.8
					$\rho(\mathrm{Cu_2Sb})$	65.0	5.4	29.6
CSS3	30.0	450	7 days	Fig. 2e	L	~11	~52	~37
					$\rho(\mathrm{Cu_2Sb})$	64.7	5.1	30.2
CSS4	37.0	450	7 days		L	~11	~55	~34
					$\rho(\mathrm{Cu_2Sb})$	65.0	6.1	28.9
CSS5	48.0	450	7 days		L	~19	~49	~32
					$\rho(\mathrm{Cu_2Sb})$	64.8	6.1	29.1
					$\varepsilon(\mathrm{Cu_3Sn})$	74.4	21.1	4.5
CSS6	50.0	450	7 days	Fig. 2d	L	~19	~49	~32
					$\rho(\mathrm{Cu_2Sb})$	64.9	6.0	29.1
					$\varepsilon(\mathrm{Cu_3Sn})$	74.5	21.0	4.5
CSS5	48.0	520	7 days		L	~39	~32	~29
					$\gamma_1\mathrm{Cu_3(Sb,Sn)}$	70.0	13.2	17.8
CSS6	50.0	520	7 days	Fig. 2f	L	~36	~34	~30
					$\gamma_1\mathrm{Cu_3(Sb,Sn)}$	70.0	13.6	16.4

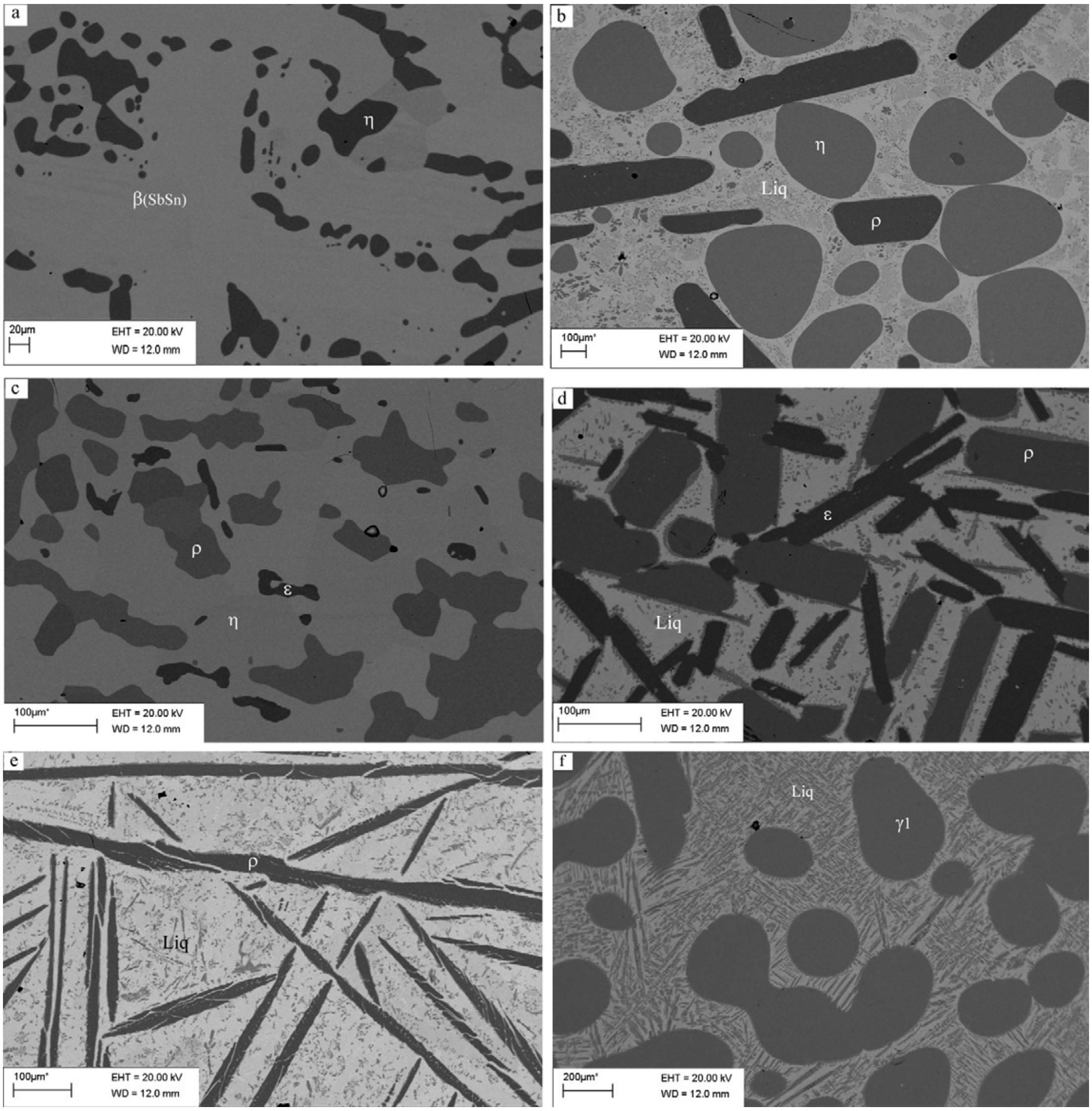

Fig. 2. (a–f) BSE images of selected Cu–Sn–Sb samples annealed at various temperatures and quenched in icy-water. In the figure the following abbreviations have been used: γ_1 for $\gamma_1 Cu_3(Sb,Sn)$, ε for $\varepsilon(Cu_3Sn)$, η for $\eta(Cu_6Sn_5)$ and ρ for $\rho(Cu_2Sb)$. (a) CSS1 annealed at 350 °C for 40 days; (b) CSS4 annealed at 380 °C for 25 days; (c) CSS7 annealed at 400 °C for 25 days; (d) CSS6 annealed at 450 °C for 7 days;(e) CSS3 annealed at 450 °C for 7 days; (f) CSS6 annealed at 520 °C for 7 days.

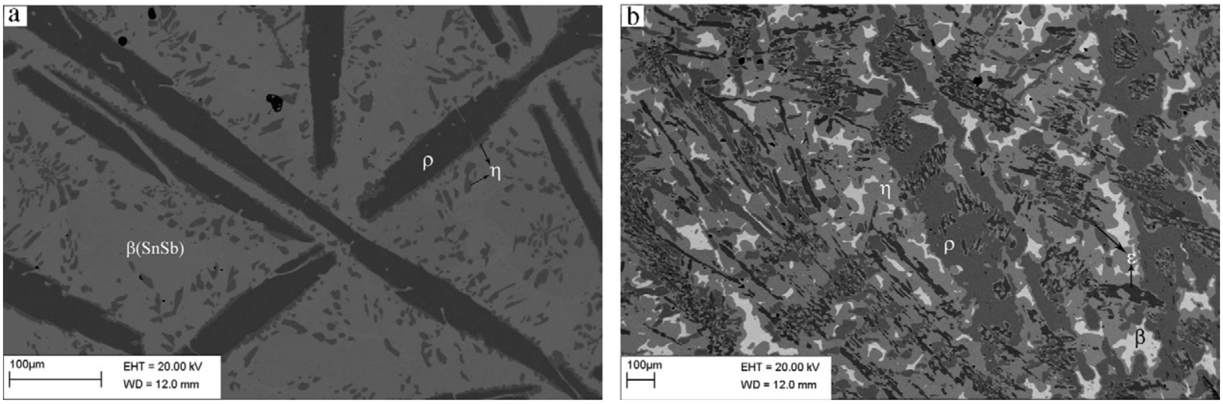

Fig. 3. BSE images of the Cu–Sn–Sb alloys: (a) as-cast CSS3 sample; (b) CSS7 sample after DSC. In the figure the following abbreviations have been used: β for β(SbSn), η for $\eta(Cu_6Sn_5)$ and ρ for $\rho(Cu_2Sb)$.

the microstructure observed in the alloys after DSC analyses (see Fig. 3b) and in the annealed specimens, as well as to the reaction scheme reported by Ghosh [9], these effects are due to the unfinished U3 reaction at 368 °C giving a remaining quantity of liquid which went through the U4 and U5 reactions. In order to confirm this assumption, we performed on the CSS1 alloy annealed at 350 °C for 40 days a DSC analysis at 0.5 °C/min rate and no thermal effects were observed in the 200–350 °C temperature range.

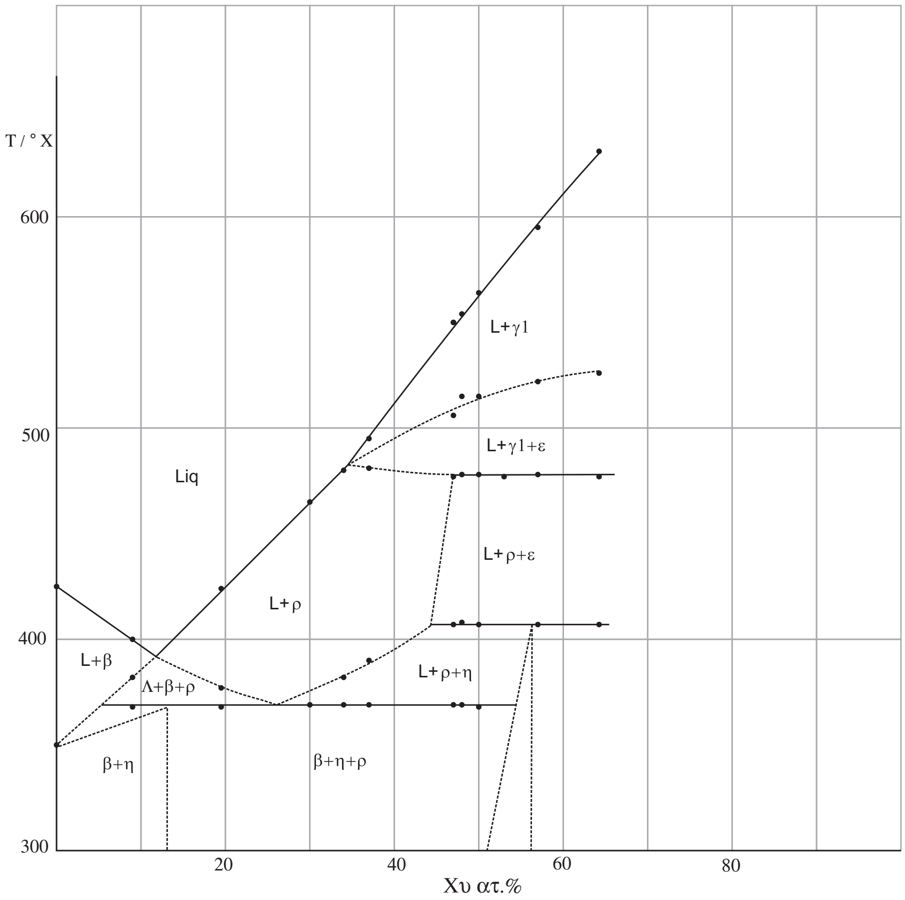

Fig. 4. Cu–Sn–Sb system. Sn:Sb = 1:1 vertical section, Cu content in at.%. Experimental DSC points are shown. In the figure the following abbreviations have been used: β for β(SbSn), γ_1 for $\gamma_1 Cu_3(Sb,Sn)$, ε for $\varepsilon(Cu_3Sn)$, η for $\eta(Cu_6Sn_5)$and ρ for $\rho(Cu_2Sb)$.

The same procedure was applied to the CSS7 sample, for which the small thermal effect at 368 °C (U3 reaction) observed in the as-cast alloy was not detected in the DSC curves of the specimen annealed 25 days at 400 °C. For the same reason, the DSC curves reported in Fig. 1b for the as cast sample CSS8, show a small effect around 368°; this is due to the remaining liquid from the unfinished U2 reaction which goes through the U3 reaction.

Combining the results obtained from DSC and SEM analyses, the phase diagram of the Cu–Sn–Sb ternary system has been established along the Sn:Sb = 1:1 isopleth section up to 65 at.% Cu and is reported in Fig. 4. It should be noticed that, the U4 and U5 reactions experimentally observed in several samples belonging to this section, as explained above are due to the unfinished U3 reaction and therefore are not inserted in the isopleth section.

Acknowledgements

This study is a contribution to the COST Action MP0602 (Advanced Solder Materials for High Temperature Application—HISOLD).

Financial support from China Scholarship Council is gratefully acknowledged.

References

[1] W. Campbell, Proc. Am. Soc. Test. Mater. 13 (1913) 630–668.
[2] F.G. Thompson, F. Orme, J. Inst. Met. 22 (1919) 203–216.
[3] O.F. Hudson, J.H. Darley, J. Inst. Met. 24 (2) (1920) 361–370.
[4] W. Bonsack, Z. Metallkd. 19 (1927) 107–110.
[5] O.W. Ellis, G.B. Karelitz, Trans. Am. Soc. Mech. Eng. 50 (11) (1928) 13–28.
[6] M. Tasaki, Mem. Coll. Eng. Kyoto Imp. Univ. A 12 (1929) 227–255.
[7] J.V. Harding, W.T. Pell-Walpole, J. Inst. Met. 75 (1948–1949) 115–130.
[8] O.J. Kleppa, J. Phys. Chem. 60 (1956) 842–846.
[9] G. Ghosh, in: G. Effenberg, S. Ilyenko (Eds.), The Landolt-Börnstein, New Series IV/11C2, pp. 420–436, SpringerMaterials – The Landolt-Börnstein Database, doi:10.1007/978-3-540-47000-7_37, http://www.springermaterials.com.
[10] J. Romanowska, Calphad 33 (2009) 723–725.
[11] D. Jendrzejczyk-Handzlik, M. Rechchach, W. Gierlotka, H. Ipser, H. Flandorfer, Enthalpies of mixing of liquid systems for lead-free soldering: Cu-Sb-Sn system, Thermochimica Acta (2010), doi:10.1016/j.tca.2010.10.010.
[12] W.J. Boettinger, U.R. Kattner, K.-W. Moon, J.H. Perepezko, DTA and Heat-flux DSC Measurements of Alloy Melting and Freezing, Natl. Inst. Stand. Technol., Washington, 2006, Spec. Publ.
[13] M. Kamal, J.C. Pieri, R. Jouty, Ann. Chim. (Paris) 4 (4) (1979) 305–311.